Published in final edited form as:
Vaccine. 2005 May 31; 23(29): 3864–3874. doi:10.1016/j.vaccine.2004.10.032.

Characterization of DNA vaccines encoding the domains of calreticulin for their ability to elicit tumor-specific immunity and antiangiogenesis

Wen-Fang Cheng[a,1], **Chien-Fu Hung**[b,1], **Chi-An Chen**[a], **Chien-Nan Lee**[a], **Yi-Ning Su**[c], **Chee-Yin Chai**[d], **David A.K. Boyd**[b], **Chang-Yao Hsieh**[a,2], and **T.-C. Wu**[b,e,f,g,*]

[a]Department of Obstetrics and Gynecology, National Taiwan University Hospital, Taipei, Taiwan

[b]Department of Pathology, The Johns Hopkins University School of Medicine, Ross 512, 720 Rutland Avenue, Baltimore, MD 21205, USA

[c]Genetic Medicine, National Taiwan University Hospital, Taipei, Taiwan

[d]Department of Pathology, School of Medicine, Kaohsiung Medical University, Kaohsiung, Taiwan

[e]Department of Obstetrics and Gynecology, Johns Hopkins Medical Institutions, Baltimore, MD, USA

[f]Department of Molecular Microbiology and Immunology, Johns Hopkins Medical Institutions, Baltimore, MD, USA

[g]Department of Oncology, Johns Hopkins Medical Institutions, Baltimore, MD, USA

Abstract

Antigen-specific cancer immunotherapy and antiangiogenesis are feasible strategies for cancer therapy because they can potentially treat systemic tumors at multiple sites in the body while discriminating between neoplastic and non-neoplastic cells. We have previously developed a DNA vaccine encoding calreticulin (CRT) linked to human papillomavirus-16 E7 and have found that this vaccine generates strong E7-specific antitumor immunity and antiangiogenic effects in vaccinated mice. In this study, we characterized the domains of CRT to produce E7-specific antitumor immunity and antiangiogenic effects by generating DNA vaccines encoding each of the three domains of CRT (N, P, and C domains) linked to the HPV-16 E7 antigen. We found that C57BL/6 mice vaccinated intradermally with DNA encoding the N domain of CRT (NCRT), the P domain of CRT (PCRT), or the C domain of CRT (CCRT) linked with E7 exhibited significant increases in E7-specific $CD8^+$ T cell precursors and impressive antitumor effects against E7-expressing tumors compared to mice vaccinated with wild-type E7 DNA. In addition, the N domain of CRT also showed antiangiogenic properties that might have contributed to the antitumor effect of NCRT/E7. Thus, the N domain of CRT can be linked to a tumor antigen in a DNA vaccine to generate both antigen-specific immunity and antiangiogenic effects for cancer therapy.

*Corresponding author. Tel.: +1 410 614 3899; fax: +1 443 287 4295. cyhsieh@ha.mc.ntu.edu.tw (C.-Y. Hsieh), wutc@jhmi.edu (T.-C. Wu).
[1]Wen-Fang Cheng and Chien-Fu Hung are equal contributors to this article.
[2]Tel.: 886 2 2312 3456; fax: 886 2 2393 4197.

Keywords

Calreticulin; DNA vaccine; NCRT; CCRT; PCRT; HPV-16; E7 antigen

1. Introduction

Antigen-specific cancer immunotherapy and antiangiogenesis are feasible strategies for cancer therapy because they are able to treat systemic tumors at multiple sites in the body while discriminating between neoplastic and non-neoplastic cells. Activation of antigen-specific T cell-mediated immune responses allows for killing of tumors associated with a specific antigen [1,2] while inhibition of angiogenesis controls neoplastic growth by sequestering neoplastic cells from an adequate blood supply [3,4]. Therefore, an innovative approach that combines both mechanisms will likely generate the most potent antitumor effect.

We have previously combined tumor-specific immunity and antiangiogenesis in an innovative DNA vaccine strategy encoding calreticulin (CRT) linked to model antigen HPV-16 E7 [5]. CRT is an abundant 46 kDa Ca^{2+}-binding protein located in the endoplasmic reticulum (ER) [6]. The protein has been shown to associate with peptides delivered into the ER by transporters associated with antigen processing (TAP-1 and TAP-2) [7] and with MHC class I-β2 microglobulin molecules to aid in antigen presentation [8]. Previous studies have shown that CRT can be complexed with peptides in vitro to elicit peptide-specific $CD8^+$ T cell responses through exogenous administration [9]. Recently, full-length calreticulin has been reported to be an endothelial cell inhibitor and exerts antitumor effects in vivo via antiangiogenesis [10–12]).

The CRT protein is composed of three domains, the N domain, P domain and C domain. The N domain (residues 1–180), also known as vasostatin, is extremely conserved among calreticulins from different species [13]. The N domain interacts with the DNA-binding domain of the glucocorticoid receptor in vitro [14], with rubella virus RNA [15], with α-integrin [16], and with protein disulphide-isomerase (PDI) and ER protein 57 (ERp57) [17]. The N domain of calreticulin also inhibits proliferation of endothelial cells and suppresses angiogenesis [10]. The P domain (residues 181–280) is rich in proline and contains two sets of three sequence repeats. This region of the protein binds Ca^{2+} with high affinity [18]. The P domain is thought to be critical for the lectin-like chaperone activity of calreticulin [19]. The P domain of calreticulin also interacts with PDI [17] and perforin [20,21]. The C-terminal region of the protein is highly acidic and terminates with the KDEL ER retrieval sequence [22]. This C domain of CRT binds to calcium [18] and to blood-clotting factors [23] and inhibits injury-induced restenosis [24].

In the present study, we investigated DNA vaccines encoding each of the N, P, and C domains of calreticulin chimerically linked to HPV-16 E7 for their abilities to elicit antigen-specific $CD8^+$ T cell responses and antitumor immunity in vaccinated mice. We found that C57BL/6 mice vaccinated intradermally with NCRT/E7, PCRT/E7 or CCRT/E7 DNA exhibited significant increases in E7-specific $CD8^+$ T cell precursors and impressive antitumor effects against E7-expressing tumors compared with mice vaccinated with wild-type E7 DNA. We also determined that the N domain of calreticulin (NCRT) resulted in antiangiogenic antitumor effects. Thus, cancer therapy using NCRT linked to a tumor antigen holds promise for treating tumors through a combination of antigen-specific immunotherapy and antiangiogenesis.

2. Materials and methods

2.1. Plasmid DNA constructs and preparation

The generation of pcDNA3-E7 has been described previously [5,25]. The generation of pcDNA3-CRT has also been described previously [5]. There is more than 90% homology between rabbit, human, mouse, and rat CRT [26]. For the generation of pcDNA3-NCRT, DNA encoding the N domain of CRT, NCRT was first amplified with PCR by using rabbit CRT cDNA as the template [27] and a set of primers, 5′-CCGG-TCTAGAATGCTGCTCCCTGTGCCGCT-3′ and 5′-CCC-GAATTCGTTGTCCGGCCGCACGATCA-3′. The amplified product was further cloned into the *Xba*1/*Eco*RI site of pcDNA3 (Invitrogen Corp., Carlsbad, CA, USA). For the generation of pcDNA3-PCRT, DNA encoding the P domain of CRT was first amplified with PCR using rabbit CRT cDNA as the template and a set of primers, 5′-TGCTCTAGAAC-GTATGAGGTGAAGATTGA-3′ and 5′-CCGGAATTCGG-GGTTCTGAATCACCGGC-3′. The amplified product was further cloned into the *Xba*I/*Eco*RI site of pcDNA3. For the generation of pcDNA3-CCRT, DNA encoding the C domain of CRT was first amplified with PCR using rabbit CRT cDNA as the template and a set of primers, 5′-TGCTCTAGAGA-GTACAAGGGTGAGTGGAAGC-3′ and 5′-CCGGAATTC-CAGCTCGTCCTTGGCCTGGC-3′. The completed product was then cloned into the *Xba*I/*Eco*RI site of pcDNA3. For the generation of pcDNA3-NCRT/E7, PCRT/E7, and CCRT/E7, E7 was first amplified with pcDNA3-E7 as a template and a set of primers, 5′-GGGGAATTCATGGAGATACACCTA-3′ and 5′-GGTGGATCCTTGAGAACAGATGG-3′, and then cloned it into the *Eco*RI/*Bam*HI sites of pcDNA3-NCRT, pcDNA3-PCRT, or pcDNA3-CCRT to generate pcDNA3-NCRT/E7, pcDNA3-PCRT/E7, or pcDNA3-CCRT/E7.

2.2. Cell line

The production and maintenance of TC-1 cells have been described previously [28]. In brief, HPV-16 E6, E7 and *ras* oncogene were used to transform primary C57BL/6 mice lung epithelial cells to generate TC-1.

2.3. DNA vaccination

Preparation of DNA-coated gold particles and gene gun particle-mediated DNA vaccinations were performed using a helium-driven gene gun according to a protocol described previously with some modifications [25]. Gene gun particle-mediated DNA vaccinations were performed using a Low Pressure-accelerated Gene Gun (BioWare Technologies Co. Ltd., Taipei, Taiwan). The gold particles (Bio-Rad 1652263) were weighted and suspended in 70% ethanol. This suspension was vortexed vigorously and then centrifuged to collect the particles. After washing by distilled water three times, the collected particles were resuspended in DNA solution (1 μg DNA per mg gold particles), vortexed and sonicated for a few seconds, and then added 2.5 M $CaCl_2$ and 0.05 M spermidine solution with vortex. This solution was kept on ice for 10 min and the DNA-coated gold particles were collected and washed by 100% ethanol three times. Finally, the particles were resuspended in 100% ethanol with appropriate concentration and used to make bullets. Control plasmid (no insert), E7, NCRT, NCRT/E7, PCRT/E7, CCRT/E7, or CRT/E7 DNA-coated gold particles were delivered to the shaved abdominal region of mice using a low pressure-accelerated Gene Gun (BioWare Technologies Co. Ltd., Taipei, Taiwan) with a 50 psi discharge pressure of helium.

2.4. Intracellular cytokine staining and flow cytometry analysis

Mice were immunized with 2 μg of the various DNA vaccines and received a booster with the same regimen 1 week later. Splenocytes were harvested 1 week after the last vaccination. Before intracellular cytokine staining, 5×10^6 pooled splenocytes from each vaccination group were incubated for 16 h with either 1 μg/ml of E7 peptide (aa 49–57) containing an MHC class I epitope [29] for detecting E7-specific $CD8^+$ T cell precursors or 10 μg/ml of E7 peptide (aa 30–67) containing an MHC class II epitope [30] for detecting E7-specific $CD4^+$ T cell precursors. Cell surface marker staining for CD8 or CD4 and intracellular cytokine staining for IFN-γ, as well as flow cytometry analysis, were performed using conditions described previously [31].

2.5. Enzyme-linked immunoabsorbent assay (ELISA) for anti-E7 antibody

For the detection of HPV 16 E7-specific antibodies in the sera, a direct ELISA was used as described previously [5]. Mice were immunized with 2 μg of the various DNA vaccines and received a booster with the same regimen 1 week later. Sera were prepared from mice on day 14 after immunization. Briefly, a 96-microwell plate was coated with 100 μl of bacteria-derived HPV-16 E7 proteins (0.5 μg/ml) and incubated at 4 °C overnight. The wells were then blocked with phosphate-buffered saline (PBS) containing 20% fetal bovine serum. Sera were prepared from mice on day 14, post immunization, serially diluted in PBS, added to the ELISA wells, and incubated at 37 °C for 2 h. After washing with PBS containing 0.05% Tween 20, the plate was incubated with a 1:2000 dilution of a peroxidase-conjugated rabbit anti-mouse IgG antibody (Zymed, San Francisco, CA) at room temperature for 1 h. The plate was washed, developed with 1-Step Turbo TMB-ELISA (Pierce, Rockford, IL), and stopped with 1 M H_2SO4. The ELISA plate was read with a standard ELISA reader at 450 nm.

2.6. In vivo tumor protection experiments

For the tumor protection experiment, C57BL/6 mice (five per group) either received no vaccination or were immunized with 2 μg/mouse of plasmid encoding no insert, NCRT, E7, NCRT/E7, PCRT/E7, CCRT/E7 or NCRT mixed with E7 using a gene gun. One week later, mice were boosted with the same regimen as the first vaccination. One week after the last vaccination, mice were subcutaneously challenged with $5 \times l0^4$ TC-1 cells/mouse in the right leg. Mice were monitored for evidence of tumor growth by palpation and inspection twice a week until they were sacrificed at day 60.

2.7. In vivo antibody depletion experiments

In vivo antibody depletions were performed as described previously [28] Briefly, C57BL/6 mice (5 per group) were vaccinated with 2 mg/mouse of NCRT/E7 DNA via gene gun, boosted 1 week later, and challenged with $5 \times l0^4$ cells/mouse TC-1 tumor cells. Depletion was started one week prior to tumor challenge. MAb GK1.5 was used for CD4 depletion, MAb 2.43 was used for CD8 depletion, and MAb PK136 was used for NK1.1 depletion. Depletion was terminated on day 60 after tumor challenge.

2.8. In vivo tumor treatment experiments

In vivo tumor treatment experiments were performed using a previously described lung hematogenous spread model [32]. C57BL/6 mice were challenged with 5×10^4 TC-1 tumor cells/mouse via tail vein injection. Nude (BALB/c *nu*/*nu*) mice (five per group) were challenged with 1×10^5 cells/mouse TC-1 tumor cells via tail vein. Two days after tumor challenge, mice received 16 μg/mouse of DNA encoding no insert, NCRT DNA, E7 DNA, NCRT/E7 DNA, PCRT/E7 DNA, CCRT/E7 DNA, or CRT/E7 DNA by a gene gun, followed by two boosters with the same regimen at one-week intervals (a total of three

shots, 48 μg DNA/mouse). Mice receiving no vaccination were used as a negative control. Mice were sacrificed and lungs were explanted on day 21 after tumor challenge. The pulmonary tumor nodules in each mouse were evaluated and counted by experimenters blinded to sample identity.

2.9. Immunohistochemical labeling for the quantitation of microvessel density

Labeling of intratumoral microvessels was performed with rat anti-mouse CD31 mAb (1:30 dilution, Bioscience), followed by VECTOR® M.O.M™. Immunodetection Kit (VECTOR; Burlingame, CA). The method for quantitating microvessel density (MVD) has been described previously [33]. Briefly, slides were prepared and examined at 20× and 100×. In each section, the three most vascularized areas were chosen. Microvessel counts were obtained at 200× and the mean number in the three fields for each tumor was calculated and referred to as the MVD count. Large vessels with thick muscular walls and lumina greater than approximately eight blood cells were excluded from the count. We counted and compared MVD in tumors of similar size to minimize the influence of tumor size on the measurements. All measurements were performed by a single pathologist, blinded to sample identity.

2.10. In vivo angiogenesis assay using Matrigel

In vivo angiogenesis was assessed using the Matrigel plug assay with a protocol similar to that described previously [5,34]. Mice were immunized with 16 μg of plasmid without insert, wild-type E7, NCRT, NCRT/E7, PCRT/E7, CCRT/E7 or CRT/E7 DNA on day 0 and received a booster with the same regimen on day 7. Matrigel (Becton Dickinson and Co., Franklin Lakes, New Jersey, USA) was mixed with heparin (final concentration of 50 U/ml), bFGF (final concentration of 20 ng/ml), and VEGF (final concentration of 200 ng/ml) at 4 °C. A total of 0.5 ml/mouse of this Matrigel mixture was injected subcutaneously into the abdominal midline of DNA-vaccinated mice on day 7. Naive mice injected with Matrigel mixed with heparin, bFGF and VEGF served as a positive control; naive mice injected with Matrigel alone were used as a negative control. Mice were euthanized on day 16. The Matrigel plugs were resected from surrounding connective tissues. Half of the Matrigel plugs were fixed in 10% formaldehyde, embedded in paraffin, sectioned, and stained with hematoxylin and eosin or Giemsa stains to calculate microvessel density. In each section, the five most vascular areas were chosen. Microvessel counts were obtained at 400×, and the mean number in the five fields for the Matrigel plugs was calculated and referred to as the MVD count. The remaining half of the Matrigel plugs was assayed for hemoglobin content according to manufacturer's instructions (Drabkin's reagent kit; Sigma Diagnostics Co., St. Louis, MO, USA).

2.11. Statistical analysis

All data expressed as means ± S.D. are representative of at least two different experiments. Data for intracellular cytokine staining with flow cytometry analysis and tumor treatment experiments were evaluated by analysis of variance (ANOVA). Comparisons between individual data points were made using a Student's *t*-test. In the tumor protection experiment, the principal outcome of interest was time to development of tumor. The event time distributions for different mice were compared by Kaplan and Meier and by log-rank analyses.

3. Results

3.1. Vaccination with DNA encoding NCRT, PCRT, or CCRT linked to E7 significantly enhances the E7-specific CD8$^+$ T cell response

A schematic diagram of the DNA constructs used in the study is shown in Fig. 1. To determine if the different domains of calreticulin when linked with the E7 DNA vaccines could enhance E7-specific T cell-mediated immune responses in mice, we performed intracellular cytokine staining with flow cytometry analysis to characterize E7-specific CD8$^+$ and CD4$^+$ T cell precursors. As shown in Fig. 2A, mice vaccinated with NCRT/E7, PCRT/E7, or CCRT/E7 DNA generated higher frequencies of E7-specific IFN-γ-secreting CD8$^+$ T cell precursors when compared to mice vaccinated with E7 DNA ($P < 0.01$). DNA encoding no insert was used as a negative control. Our results also indicated that the physical linkage of NCRT to E7 was required for enhancement of CD8$^+$ T cell activity, since DNA encoding the N domain of CRT mixed with E7 DNA did not generate enhancement of CD8$^+$ T cell activity (data not shown). Vaccination with CRT/E7 DNA generated a slightly higher number of E7-specific CD8$^+$ T cell precursors (220.5 ± 18.5) compared to NCRT/E7 (178.0 ± 18.5), PCRT/E7 (140.0 ± 16.0) and CCRT/E7 (128.0 ± 10.0) ($P < 0.01$). Thus, our data suggest that NCRT/E7, PCRT/E7, and CCRT/E7 DNA vaccines are capable of enhancing the E7-specific CD8$^+$ T cell response in vaccinated mice, although not as strongly as CRT/E7.

We further evaluated whether CRT, NCRT, PCRT, or CCRT could enhance the E7-specific CD4$^+$ T cell response when linked to E7 in a DNA vaccine. DNA encoding no insert was used as a negative control. Mick-2 cells were used as a positive control and generated IFN-γ-secreting CD4$^+$ T cells in mice (data not shown). As shown in Fig. 2B, we observed no increase in the number of E7-specific IFN-γ-secreting CD4$^+$ T cells in mice vaccinated with NCRT/E7, PCRTE7, CCRT/E7, or CRT/E7 DNA compared to mice vaccinated with control plasmid, E7, or NCRT DNA (Fig. 2B).

3.2. Vaccination with NCRT/E7 DNA significantly enhances the E7-specific antibody response

We performed ELISA to determine if vaccination with NCRT/E7, PCRT/E7, or CCRT/E7 DNA could enhance E7-specific antibody responses in vaccinated mice compared to vaccination with wild-type E7 DNA. As shown in Fig. 2C, vaccination with NCRT/E7 or CRT/E7 DNA generated significantly higher titers of anti-E7 antibodies in the sera of mice compared with the other vaccinated groups ($P < 0.01$). There was no significant difference between the titers of E7 antibody generated by NCRT/E7 and CRT/E7. Our results indicated that the fusion of NCRT to E7 could enhance the E7-specific antibody response compared to wild-type E7 and that the titer of E7-specific antibody generated by the NCRT/E7 DNA vaccine is comparable to that generated by the CRT/E7 DNA vaccine.

3.3. Vaccination with NCRT/E7, PCRT/E7, or CCRT/E7 DNA enhances tumor protection in mice challenged with an E7-expressing tumor cell line

To determine if the observed enhancement of the E7-specific CD8$^+$ T cell response translated into a significant E7-specific protective antitumor effect, we performed an in vivo tumor protection experiment using a previously characterized E7-expressing tumor model, TC-1 [28]. As shown in Fig. 3, 100% of mice receiving PCRT/E7, CCRT/E7, or CRT/E7 DNA vaccination also remained tumor-free 60 days after TC-1 challenge. In comparison, all mice vaccinated with wild-type E7 DNA developed tumors within 14 days of challenge. This suggests that each of the three domains of calreticulin can protect vaccinated mice against a lethal challenge with E7-expressing tumor cells when linked to the E7 antigen in a DNA vaccine.

3.4. Treatment with NCRT/E7, PCRT/E7, or CCRT/E7 DNA leads to significant reduction of pulmonary tumor nodules in C57BL/6 wild-type mice

We further assessed the therapeutic potential of each vaccine by performing an in vivo tumor treatment experiment using a previously described lung hematogenous spread model [5]. As shown in Fig. 4, C57BL/6 mice treated with NCRT/E7 DNA (1.0 ± 0.4), PCRT/E7 (1.2 ± 0.8), or CCRT/E7 (1.4 ± 0.6) all exhibited significantly fewer pulmonary tumor nodules than mice treated with the other DNA vaccines (wild-type E7 (139.0 ± 11.0) or NCRT (34.0 ± 3.2) did (one-way ANOVA, $P < 0.001$). These data indicated that any of the three domains of calreticulin, when linked with E7 antigen, could generate more potent antitumor effects than wild-type E7 DNA constructs in a lung hematogenous spread model.

We also observed that treatment of mice with NCRT DNA also resulted in significantly fewer tumor nodules than treatment with wild-type E7 DNA or no treatment (one-way ANOVA, $P < 0.001$). This suggests that NCRT may generate an antitumor effect that is independent of antigen-specific T cell-mediated immunity.

3.5. Treatment with NCRT/E7 or NCRT DNA leads to significant reduction of pulmonary tumor nodules in immunocompromised mice

To confirm that treatment with NCRT, NCRT/E7, or CRT/E7 DNA could generate a T cell-independent antitumor effect, we performed an in vivo tumor treatment experiment using immunocompromised (BALB/c *nu*/*nu*) mice. As shown in Fig. 5A, nude mice treated with NCRT, NCRT/E7, or CRT/E7 DNA displayed a significantly lower mean number of pulmonary tumor nodules (18.0 ± 2.0 for NCRT, 25.0 ± 4.0 for NCRT/E7) compared with mice treated with wild-type E7 DNA (215.0 ± 10.0), plasmid without insert (217.5 ± 17.0), or naive group (230.0 ± 22.5) (one-way ANOVA, $P < 0.001$). Interestingly, no significant reduction in tumor nodules could be detected in mice treated with PCRT/E7 or CCRT/E7 compared to mice treated with wild-type E7. In addition, nude mice treated with NCRT/E7 DNA exhibited significantly fewer pulmonary tumor nodules than nude mice treated with CRT/E7 DNA (one-way ANOVA, $P < 0.05$). Our data suggest that treatment with NCRT, NCRT/E7, or CRT/E7 DNA are able to generate an antitumor effect even in the absence of T cell-mediated immune responses and that PCRT/E7 and CCRT/E7 DNA are not able to do this.

3.6. Tumors from BALB/c nude mice treated with NCRT, NCRT/E7, or CRT/E7 DNA show a reduction in microvessel density (MVD)

To determine whether the antitumor effect of NCRT, NCRT/E7, or CRT/E7 DNA in the absence of T cells might be mediated through antiangiogenesis, we measured MVD in the pulmonary tumors of nude mice treated with various DNA vaccines. As shown in Fig. 5B, treatment of nude mice with NCRT, NCRT/E7, or CRT/E7 DNA resulted in significantly lower MVD in pulmonary tumors than treatment with wild-type E7, PCRT/E7 or CCRT/E7 group (one-way ANOVA, $P < 0.001$). MVD in pulmonary tumors was significantly lower in nude mice treated with NCRT/E7 DNA than in nude mice treated with CRT/E7 DNA (one-way ANOVA, $P < 0.05$). Taken together, our data suggest that the T cell-independent antitumor effect elicited by vaccination with NCRT, NCRT/E7, or CRT/E7 DNA is antiangiogenic and that this angiogenic effect may be related to the N domain of CRT.

3.7. Matrigels from C57BL/6 mice challenged with TC-1 and treated with NCRT, NCRT/E7, or CRT/E7 DNA show reduced microvessel density and hemoglobin content

To provide a more quantitative assessment of antiangiogenesis in C57BL/6 mice treated with the various DNA constructs, we performed an in vivo angiogenesis assay using Matrigel [5]. As shown in Fig. 6A, the hemoglobin contents of Matrigel implants from

NCRT, NCRT/E7, or CRT/E7-treated mice were significantly lower than those from mice treated with DNA encoding no insert, E7, PCRT/E7, or CCRT/E7 ($P < 0.01$, ANOVA). This assay revealed that NCRT or NCRT/E7 DNA could generate a similar degree of inhibition of bFGF- and VEGF-induced in vivo angiogenesis. Interestingly, the hemoglobin contents of Matrigel implants from NCRT/E7-treated mice were significantly lower than those from CRT/E7-treated mice ($P < 0.01$, ANOVA). We also examined the MVD of Matrigel samples to provide another measure of angiogenesis inhibition, since red blood cells may extravasate from vessels and affect the hemoglobin count. As seen in Fig. 6B, the mean MVDs in Matrigel samples from NCRT (23.7 ± 10.4), NCRT/E7 (21.3 ± 4.7), and CRT/E7 (29.0 ± 9.2) DNA-treated mice were similar and significantly lower than the MVDs in Matrigel samples from no insert (98.3 ± 31.8), wild-type E7 (76.7 ± 12.0), CCRT/E7 (77.3 ± 9.6), or PCRT/E7 (76.3 ± 6.7) DNA-treated mice. Thus, our data confirm that the N domain of CRT is responsible for the antiangiogenic effect observed in mice treated with CRT/E7.

3.8. Linkage of NCRT to E7 is essential for generating the antitumor effect against TC-1 cells in vaccinated mice

To assess whether the linkage of NCRT to E7 is essential for the antitumor effect against E7-expressing tumors in vaccinated mice, we performed in vivo tumor protection experiments using TC-1 tumor cells. Mice were vaccinated with various DNA constructs, including E7 DNA, NCRT DNA, NCRT/E7, and NCRT DNA mixed with E7 DNA. One week after the last vaccination, mice were challenged with $5 \times l0^4$/mouse of TC-1 cells. As shown in Fig. 7A, all mice vaccinated with the NCRT/E7 DNA vaccine remained tumor-free. In contrast, all mice vaccinated with the other DNA vaccines (including NCRT mixed with E7) developed tumors within 2 weeks after challenge with TC-1 cells. Our results indicate that the linkage of NCRT to E7 was essential for the observed antitumor effects in the vaccinated mice.

3.9. $CD8^+$ T cells, but not $CD4^+$ T cells or NK cells, are important for the antitumor effect generated by the NCRT/E7 DNA vaccine

To determine the subset of lymphocytes that is important for the antitumor effect generated by the NCRT/E7 DNA vaccine, we performed in vivo antibody depletion experiments. As shown in Fig. 7B, all NCRT/E7 DNA-vaccinated mice depleted of $CD8^+$ T cells and all unvaccinated naive mice grew tumors within 14 days after tumor challenge. In contrast, all NCRT/E7 DNA-vaccinated mice depleted of $CD4^+$ T cells and NK cells remained tumor free 56 days after tumor challenge. These results suggest that $CD8^+$ T cells, but not $CD4^+$ T cells or NK cells, were essential for the antitumor immunity generated by the NCRT/E7 DNA vaccine.

4. Discussion

In this study, we demonstrated that linkage of NCRT, PCRT, or CCRT to the HPV-16 E7 antigen can significantly enhance the potency of an E7-expressing DNA vaccine. All three domains of calreticulin linked with E7 DNA elicited strong E7-specific $CD8^+$ T cell immune responses, generated significant $CD8^+$ T cell-dependent protective effects against subcutaneous HPV-16 E7-expressing tumors, and could effectively treat lethal pulmonary tumor nodules. In comparison, vaccination with only NCRT/E7 or CRT/E7 DNA was able to significantly enhance the E7-specific antibody response when compared to the other DNA vaccine constructs. Furthermore, only DNA vaccines encoding the N domain of CRT generated a therapeutic effect due to inhibition of angiogenesis, which likely contributed to reduction of pulmonary tumor nodules. Thus, a DNA vaccine encoding NCRT chimerically linked to a tumor antigen represents another valid approach combining immunological and antiangiogenic approaches for the generation of a potent antitumor effect.

Our data demonstrated that all three domains of calreticulin could enhance the E7-specific $CD8^+$ T cell immune response when linked with the HPV-16 E7 antigen. It has been previously shown that professional APCs, directly transfected via gene gun, play a primary role in eliciting an antigen-specific T cell response to DNA vaccination [35]. Full length CRT has been shown to be able to enhance MHC class I processing of antigen by targeting linked antigen to the ER [5]. One or more domains of CRT may also enhance MHC class I processing of the linked E7 antigen in transfected professional APCs. Another mechanism that may play a role in the enhancement of E7-specific $CD8^+$ T cell immune responses in vivo is the so-called "cross-priming" effects, whereby secretion of chimeric protein or lysis of cells expressing chimeric antigen releases the chimeric protein exogenously to be taken up and processed by other APCs via the MHC class I restricted pathways. CD91, an α2 macroglobulin receptor, serves as a receptor for heat shock proteins, including calreticulin, gp96, HSP70 and HSP90 and facilitate the cross-priming effects [9]. It is still uncertain which of the three domains of CRT is capable of binding with CD91. These direct and cross-priming mechanisms may provide some explanation for the observed enhancement of E7-specific $CD8^+$ T cell activity in mice vaccinated with NCRT/E7, PCRT/E7 or CCRT/E7 DNA.

Out of the three domains of CRT, we observed that E7-specific antibody titers were significantly enhanced by NCRT/E7 vaccination only. This may be due to the fact that NCRT encodes the signal sequence of CRT, allowing extracellular secretion and stimulation of B cells by NCRT/E7. Vaccination with PCRT/E7 or CCRT/E7 DNA may not have been capable of eliciting an E7-specific Ab response because they lack this sequence. To address if T cells are required for the observed E7-specific antibody response, we have used immunocompromised mice (BALB/c *nu/nu*) for our studies. Our data indicate that nude mice vaccinated with CRT/E7 are capable of generating an E7-specific antibody response (data not shown), suggesting that the antibody response mediated by calreticulin may be contributed by T cell independent mechanisms. Even though antibody-mediated responses have not been shown to play an important role in controlling HPV-associated malignancies, antigen-specific Abs are significant in other tumor models, such as the breast cancer model with the HER-2/neu antigen. The chimeric NCRT or CRT vaccine strategy may be used to generate HER-2/neuspecific Ab's to induce growth arrest in cells expressing high levels of HER-2/neu on the cell surface [36].

We observed that treatment of immunocompromised mice (BALB/c *nu/nu*) with NCRT/E7 or NCRT DNA generated comparable T cell-independent antitumor effects. Meanwhile, tumor treatment experiments and examination of microvessel density in nude mice and Matrigel experiments in C57BL/6 mice revealed that NCRT/E7 DNA generated a stronger antiangiogenic effect than CRT/E7 DNA. NCRT, the N-terminal domain of calreticulin, has been demonstrated to inhibit endothelial cell proliferation in response to bFGF or VEGF and angiogenesis in vivo [10,11]. By inhibiting endothelial cell growth, NCRT would likely reduce tumor neovascularization to inhibit tumor growth. The NCRT and NCRT/E7 DNA vaccines both showed T-cell independent antitumor effects. Thus, it seems likely that NCRT/E7 and CRT/E7 are two chimeric molecules that can control established tumors through E7-specific $CD8^+$ T cell-mediated immune responses and inhibit the growth of tumor vasculature through antiangiogenesis.

In order to generate an effective antiangiogenic antitumor effect, it is necessary to administer CRT or NCRT DNA repeatedly at high doses. Previous studies have indicated that single DNA vaccination results in peak serum CRT levels at 7 days post vaccination, tapering off to near-baseline levels within 14 days post vaccination [37]. In addition, the level of serum CRT depends on the dose of CRT DNA [37]. Typical DNA vaccine doses (2 μg) did not show any detectable serum CRT. We have used repeated, high-dose, CRT DNA

vaccination to generate detectable levels of serum CRT and antiangiogenic effects in vaccinated mice [5]. Thus, for an effective antiangiogenic antitumor response, a relatively high and repeated dose of CRT DNA is required.

The antiangiogenic property of a NCRT- or CRT-encoding DNA vaccine raises certain safety concerns. For example, wound healing requires neovascularization, which may be inhibited by angiogenesis inhibitors. However, prior studies have shown that CRT does not impair wound healing at tumor-inhibiting doses [38]. Furthermore, we have conducted experiments showing that vaccination with the CRT/E7 DNA vaccine does not inhibit wound healing or result in pathologic changes in the major organs of mice (data not shown). Thus, concerns for inhibition of wound healing after therapeutic doses of DNA encoding CRT or NCRT are likely minimal and should not inhibit clinical translation of antiangiogenic DNA vaccines encoding CRT or NCRT.

In summary, our results indicate that fusion of NCRT, PCRT or CCRT to HPV-16 E7 can generate an impressive antitumor effect against HPV-16 E7-expressing murine tumors through enhancement of E7-specific $CD8^+$ T cell-mediated immune responses. However, only NCRT/E7 can generate antitumor effect through both E7-specific $CD8^+$ T cell-mediated immune responses and antiangiogenesis, as CRT/E7 does. Thus, the fusion of NCRT to an antigen gene is a promising approach to cancer therapy that potentially can be applied to other cancer systems with known tumor-specific antigens.

Acknowledgments

We would like to thank Ken-Yu Lin and Dr. Richard Roden for critical review of the manuscript. This study was supported by grants from the National Cancer Institute and American Cancer Society.

References

1. Boon T, Cerottini JC, Van den Eynde B, van der Bruggen P, Van Pel A. Tumor antigens recognized by T lymphocytes. Ann Rev Immunol. 1994; 12:337–65. [review]. [PubMed: 8011285]
2. Chen CH, Wu TC. Experimental vaccine strategies for cancer immunotherapy. J Biomed Sci. 1998; 5(4):231–52. [PubMed: 9691216]
3. Folkman J. Angiogenesis: initiation and control. Ann N Y Acad Sci. 1982; 401:212–27. [PubMed: 6188401]
4. Hanahan D, Folkman J. Patterns and emerging mechanisms of the angiogenic switch during tumorigenesis. Cell. 1996; 86(3):353–64. [PubMed: 8756718]
5. Cheng WF, Hung CF, Chai CY, et al. Tumor-specific immunity and antiangiogenesis generated by a DNA vaccine encoding calreticulin linked to a tumor antigen. J Clin Invest. 2001; 108(5):669–78. [PubMed: 11544272]
6. Nash PD, Opas M, Michalak M. Calreticulin: not just another calcium-binding protein. Mol Cell Biochem. 1994; 135(1):71–8. [PubMed: 7816058]
7. Spee P, Neefjes J. TAP-translocated peptides specifically bind proteins in the endoplasmic reticulum, including gp96, protein disulfide isomerase and calreticulin. Eur J Immunol. 1997; 27(9): 2441–9. [PubMed: 9341791]
8. Sadasivan B, Lehner PJ, Ortmann B, Spies T, Cresswell P. Roles for calreticulin and a novel glycoprotein, tapasin, in the interaction of MHC class I molecules with TAP. Immunity. 1996; 5(2): 103–14. [PubMed: 8769474]
9. Basu S, Srivastava PK. Calreticulin, a peptide-binding chaperone of the endoplasmic reticulum, elicits tumor- and peptide-specific immunity. J Exp Med. 1999; 189(5):797–802. [PubMed: 10049943]
10. Pike SE, Yao L, Jones KD, et al. Vasostatin, a calreticulin fragment, inhibits angiogenesis and suppresses tumor growth. J Exp Med. 1998; 188(12):2349–56. [PubMed: 9858521]

11. Pike SE, Yao L, Setsuda J, et al. Calreticulin and calreticulin fragments are endothelial cell inhibitors that suppress tumor growth. Blood. 1999; 94(7):2461–8. [PubMed: 10498619]
12. Yao L, Pike SE, Tosato G. Laminin binding to the calreticulin fragment vasostatin regulates endothelial cell function. J Leukoc Biol. 2002; 71(1):47–53. [PubMed: 11781379]
13. Krause KH, Michalak M. Calreticulin. Cell. 1997; 88(4):439–43. [PubMed: 9038335]
14. Burns K, Duggan B, Atkinson EA, et al. Modulation of gene expression by calreticulin binding to the glucocorticoid receptor. Nature. 1994; 367(6462):476–80. [PubMed: 8107808]
15. Singh NK, Atreya CD, Nakhasi HL. Identification of calreticulin as a rubella virus RNA binding protein. Proc Natl Acad Sci USA. 1994; 91(26):12770–4. [PubMed: 7809119]
16. Rojiani MV, Finlay BB, Gray V, Dedhar S. In vitro interaction of a polypeptide homologous to human Ro/SS-A antigen (calreticulin) with a highly conserved amino acid sequence in the cytoplasmic domain of integrin alpha subunits. Biochemistry. 1991; 30(41):9859–66. [PubMed: 1911778]
17. Corbett EF, Oikawa K, Francois P, et al. Ca^{2+} regulation of interactions between endoplasmic reticulum chaperones. J Biol Chem. 1999; 274(10):6203–11. [PubMed: 10037706]
18. Baksh S, Michalak M. Expression of calreticulin in *Escherichia coli* and identification of its Ca^{2+} binding domains. J Biol Chem. 1991; 266(32):21458–65. [PubMed: 1939178]
19. Vassilakos A, Michalak M, Lehrman MA, Williams DB. Oligosaccharide binding characteristics of the molecular chaperones calnexin and calreticulin. Biochemistry. 1998; 37(10):3480–90. [PubMed: 9521669]
20. Andrin C, Pinkoski MJ, Burns K, et al. Interaction between a Ca^{2+}-binding protein calreticulin and perforin, a component of the cytotoxic T-cell granules. Biochemistry. 1998; 37(29):10386–94. [PubMed: 9671507]
21. Fraser SA, Michalak M, Welch WH, Hudig D. Calreticulin, a component of the endoplasmic reticulum and of cytotoxic lymphocyte granules, regulates perforin-mediated lysis in the hemolytic model system. Biochem Cell Biol. 1998; 76(5):881–7. [PubMed: 10353724]
22. Michalak M, Burns K, Andrin C, et al. Endoplasmic reticulum form of calreticulin modulates glucocorticoid-sensitive gene expression. J Biol Chem. 1996; 271(46):29436–45. [PubMed: 8910610]
23. Kuwabara K, Pinsky DJ, Schmidt AM, et al. Calreticulin, an antithrombotic agent which binds to vitamin K-dependent coagulation factors, stimulates endothelial nitric oxide production, and limits thrombosis in canine coronary arteries. J Biol Chem. 1995; 270(14):8179–87. [PubMed: 7713923]
24. Dai E, Stewart M, Ritchie B, et al. Calreticulin, a potential vascular regulatory protein, reduces intimal hyperplasia after arterial injury. Arterioscler Thromb Vasc Biol. 1997; 17(11):2359–68. [PubMed: 9409202]
25. Hung C-F, Cheng W-F, Chai C-Y, et al. Improving vaccine potency through intercellular spreading and enhanced MHC class I presentation of antigen. J Immunol. 2001; 166:5733–40. [PubMed: 11313416]
26. Michalak M, Corbett EF, Mesaeli N, Nakamura K, Opas M. Calreticulin: one protein, one gene, many functions. Biochem J. 1999; 344(Pt 2):281–92. [PubMed: 10567207]
27. Michalak M, Mariani P, Opas M. Calreticulin, a multifunctional Ca^{2+} binding chaperone of the endoplasmic reticulum. Biochem Cell Biol. 1998; 76(5):779–85. [PubMed: 10353711]
28. Lin K-Y, Guarnieri FG, Staveley-O'Carroll KF, et al. Treatment of established tumors with a novel vaccine that enhances major histocompatibility class II presentation of tumor antigen. Cancer Res. 1996; 56:21–6. [PubMed: 8548765]
29. Feltkamp MC, Smits HL, Vierboom MP, et al. Vaccination with cytotoxic T lymphocyte epitope-containing peptide protects against a tumor induced by human papillomavirus type 16-transformed cells. Eur J Immunol. 1993; 23(9):2242–9. [PubMed: 7690326]
30. Tindle RW, Croft S, Herd K, et al. A vaccine conjugate of 'ISCAR' immunocarrier and peptide epitopes of the E7 cervical cancer-associated protein of human papillomavirus type 16 elicits specific Th1- and Th2-type responses in immunized mice in the absence of oil-based adjuvants. Clin Exp Immunol. 1995; 101(2):265–71. [PubMed: 7544248]
31. Cheng WF, Hung CF, Hsu KF, et al. Cancer immunotherapy using Sindbis virus replicon particles encoding a VP22-antigen fusion. Hum Gene Ther. 2002; 13(4):553–68. [PubMed: 11874633]

32. Ji H, Wang T-L, Chen C-H, et al. Targeting HPV-16 E7 to the endosomal/lysosomal compartment enhances the antitumor immunity of DNA vaccines against murine HPV-16 E7-expressing tumors. Hum Gene Ther. 1999; 10(17):2727–40. [PubMed: 10584920]

33. Cheng WF, Lee CN, Chu JS, et al. Vascularity index as a novel parameter for the in vivo assessment of angiogenesis in patients with cervical carcinoma. Cancer. 1999; 85(3):651–7. [PubMed: 10091738]

34. Coughlin CM, Salhany KE, Wysocka M, et al. Interleukin-12 and interleukin-18 synergistically induce murine tumor regression which involves inhibition of angiogenesis. J Clin Invest. 1998; 101(6):1441–52. [PubMed: 9502787]

35. Porgador A, Irvine KR, Iwasaki A, Barber BH, Restifo NP, Germain RN. Predominant role for directly transfected dendritic cells in antigen presentation to CD8+ T cells after gene gun immunization. J Exp Med. 1998; 188(6):1075–82. [PubMed: 9743526]

36. Harwerth IM, Wels W, Schlegel J, Muller M, Hynes NE. Monoclonal antibodies directed to the erbB-2 receptor inhibit in vivo tumour cell growth. Br J Cancer. 1993; 68(6):1140–5. [PubMed: 7903153]

37. Xiao F, Wei Y, Yang L, et al. A gene therapy for cancer based on the angiogenesis inhibitor, vasostatin. Gene Ther. 2002; 9(18):1207–13. [PubMed: 12215887]

38. Lange-Asschenfeldt B, Velasco P, Streit M, et al. The angiogenesis inhibitor vasostatin does not impair wound healing at tumor-inhibiting doses. J Invest Dermatol. 2001; 117(5):1036–41. [PubMed: 11710910]

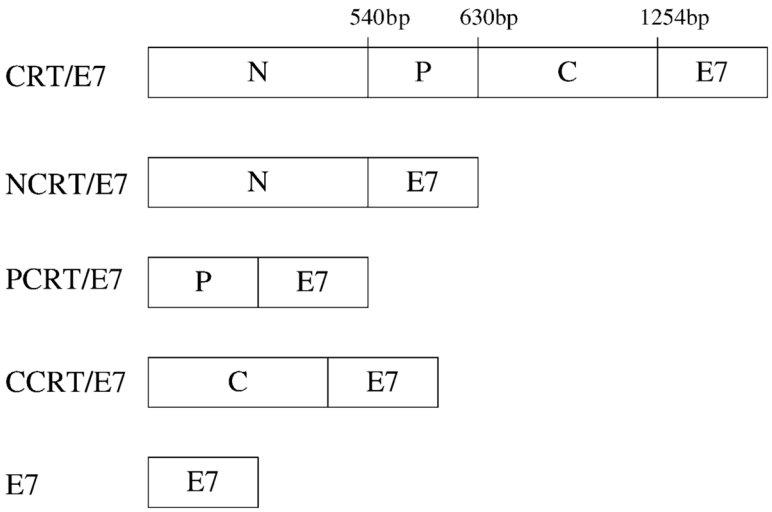

Fig. 1.

Diagram depicting the composition of the various DNA constructs used in the study. CRT is composed of three identified domains: N (1–540 bp), P (541–807 bp), and C (808–1256 bp). DNA constructs were generated to encode each of these domains linked to HPV-16 E7.

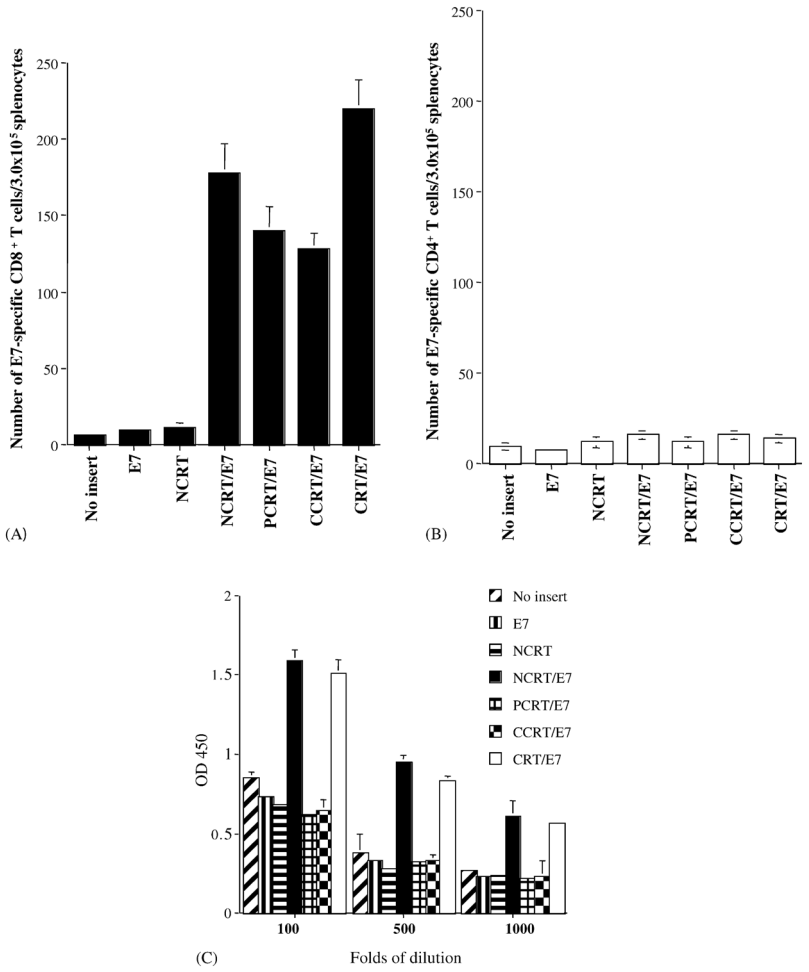

Fig. 2.

Immunological profile of vaccinated mice using intracellular cytokine staining and flow cytometry analysis and ELISA. Mice were vaccinated with DNA encoding no insert, E7, NCRT, NCRT/E7, CCRT/E7, PCRT/E7, or CRT/E7. Splenocytes from vaccinated mice were harvested 7 days after vaccination, cultured in vitro with MHC class I-restricted (aa 49–57) or class II-restricted (aa 30–67) E7 peptide overnight, and stained for intracellular IFN-γ and CD4 or CD8. (A) Bar graph depicting the number of antigen specific IFN-γ-secreting $CD8^+$ T cell precursors/3 × 10^5 splenocytes (mean ± S.D.). (B) Bar graph depicting the number of antigen specific IFN-γ-secreting $CD4^+$ T cell precursors/3 × 10^5 splenocytes (mean ± S.D.). *Note:* Mice vaccinated with CRT/E7, NCRT/E7, PCRT/E7, or CCRT/E7 DNA generated higher numbers of E7-specific IFN-γ-secreting $CD8^+$ T cell precursors than the other vaccination groups. (C) Bar graph demonstrating E7-specific antibodies in mice vaccinated with various DNA vaccines. The results from the 1:100, 1:500, and 1:1,000 dilution are presented, showing mean absorbance (OD450 nm) ± S.D. All data above are from one representative experiment of two performed. *Note:* NCRT/E7 DNA and CRT/E7 vaccines generated significantly higher E7-specific antibody responses when compared with mice vaccinated with the other DNA vaccines ($P < 0.01$, one-way ANOVA).

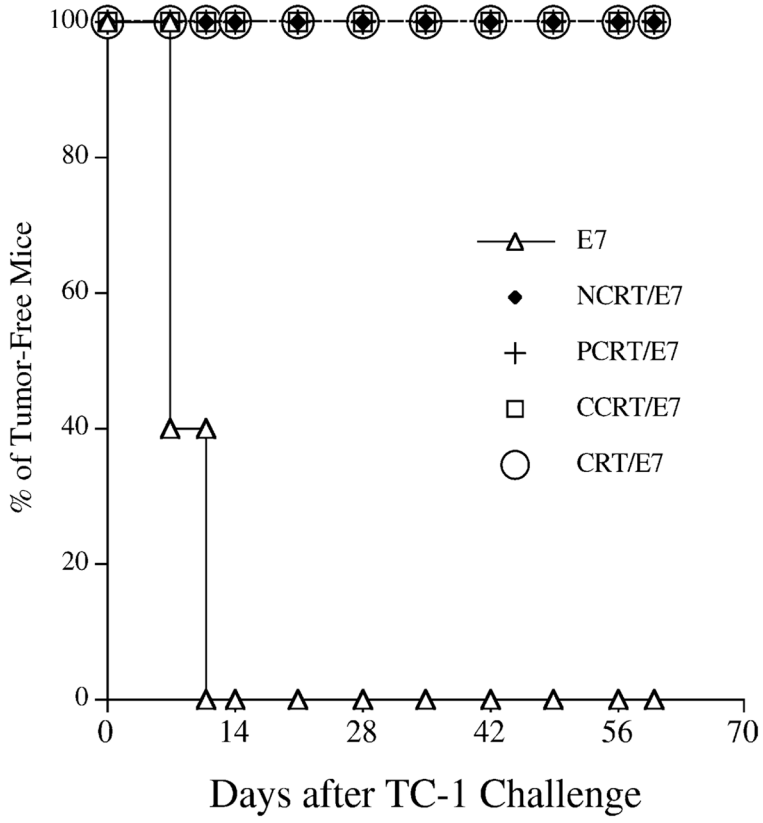

Fig. 3.

In vivo tumor protection experiments in mice vaccinated with various DNA vaccines. Mice were immunized with DNA vaccines encoding E7, NCRT/E7, PCRT/E7, CCRT/E7 or CRT/E7 and then were challenged with TC-1 tumor cells. *Note:* 100% of mice receiving NCRT/E7, PCRT/E7 CCRT/E7, or CRT/E7 remained tumor-free 60 days after TC-1 challenge.

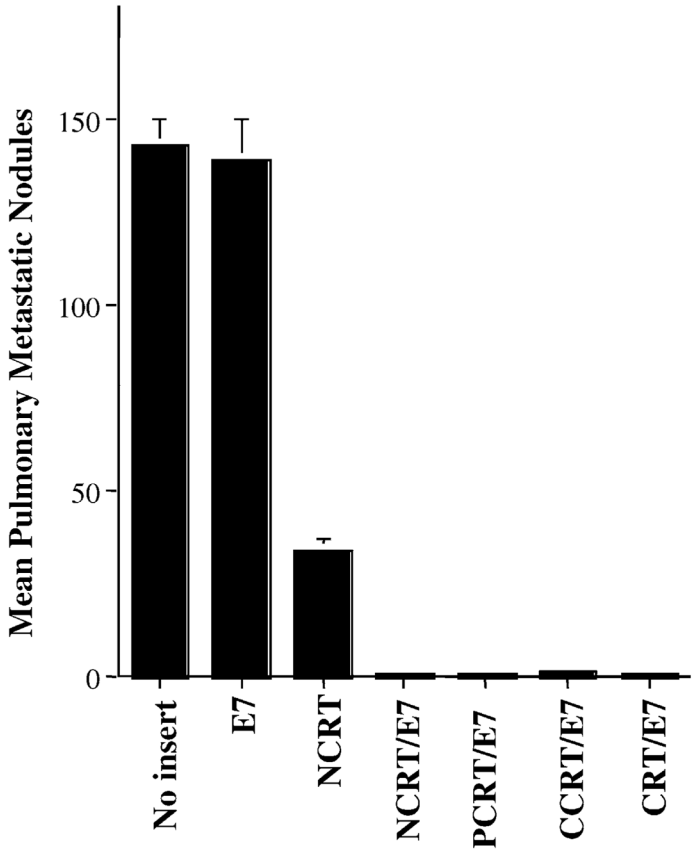

Fig. 4.

In vivo tumor treatment experiments in C57BL/6 mice. Bar graph depicting mean pulmonary tumor nodules in each vaccinated group. Mice were challenged with TC-1 tumor cells and subsequently treated with DNA encoding no insert, E7, NCRT, NCRT/E7, PCRT/E7, CCRT/E7, or CRT/E7 at a high therapeutic dose. The data are expressed as mean number of pulmonary tumor nodules ± S.D. *Note:* Mice treated with DNA encoding NCRT/E7, PCRT/E7, CCRT/E7, or CRT/E7 showed similar numbers of tumor nodules, all significantly lower than numbers in mice treated with DNA encoding E7, no insert, or NCRT.

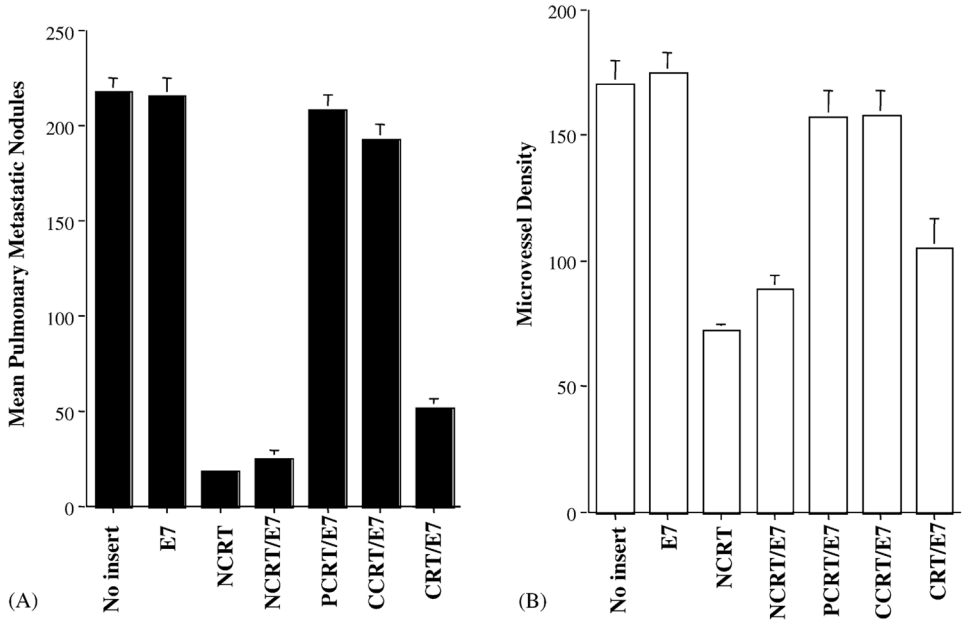

Fig. 5.

In vivo tumor treatment experiments in nude mice and the microvessel density of pulmonary tumor nodules in DNA-treated nude mice. (A) Bar graph depicting mean numbers of pulmonary tumor nodules in treated BALB/c (*nu*/*nu*) mice. Mice were challenged with TC-1 tumor cells and were subsequently treated with the various DNA vaccines at a high therapeutic dose. *Note:* Nude mice treated with NCRT, NCRT/E7 or CRT/E7 DNA vaccines showed significantly lower numbers of pulmonary tumor nodules compared with the wild-type E7, PCRT/E7 or CCRT/E7 DNA groups. (B) Bar graph depicting mean microvessel density in pulmonary tumor nodules in mice treated with the various DNA constructs. Immunohistochemical labeling and microvessel counts were performed. *Note:* The MVDs of the pulmonary tumor nodules in the NCRT, NCRT/E7, and CRT/E7 groups were significantly lower than the wild-type E7, PCRT/E7 or CCRT/E7 groups.

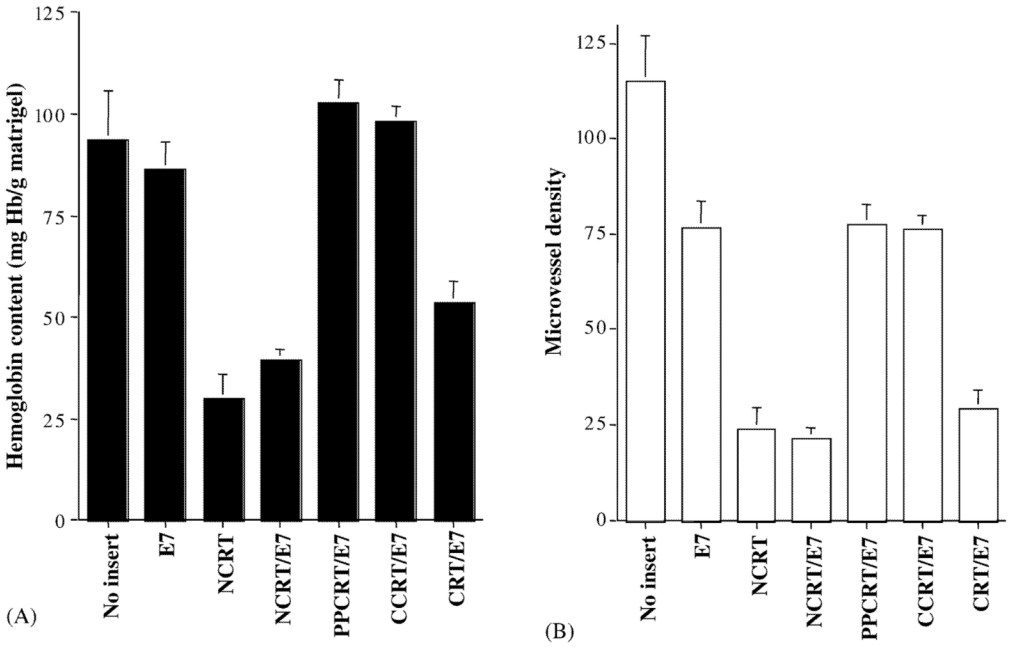

Fig. 6.

In vivo angiogenesis assay using Matrigel to characterize the antiangiogenic effect resulting from treatment with the various DNA constructs. Mice were treated with various DNA constructs and injected with Matrigel. Nine days later, mice were euthanized, and Matrigel plugs were resected. (A) Bar graph depicting Matrigel hemoglobin content for mice treated with DNA vaccines. *Note:* The NCRT, NCRT/E7, and CRT/E7 groups had lower hemoglobulin concentrations compared to the wild-type E7, PCRT/E7, and CCRT/E7 groups. (B) Bar graph displaying microvessel density of the Matrigel in mice treated with various DNA vaccines. The Matrigel plugs were fixed, embedded, sectioned, and stained to calculate microvessel density. *Note:* The mean numbers of MVD in Matrigel samples from NCRT, NCRT/E7 or CRT/E7 DNA-treated mice were similar and significantly lower than those of the MVD in Matrigel samples from pcDNA3 without insert, wild-type E7, CCRT/E7, or PCRT/E7 DNA-treated mice.

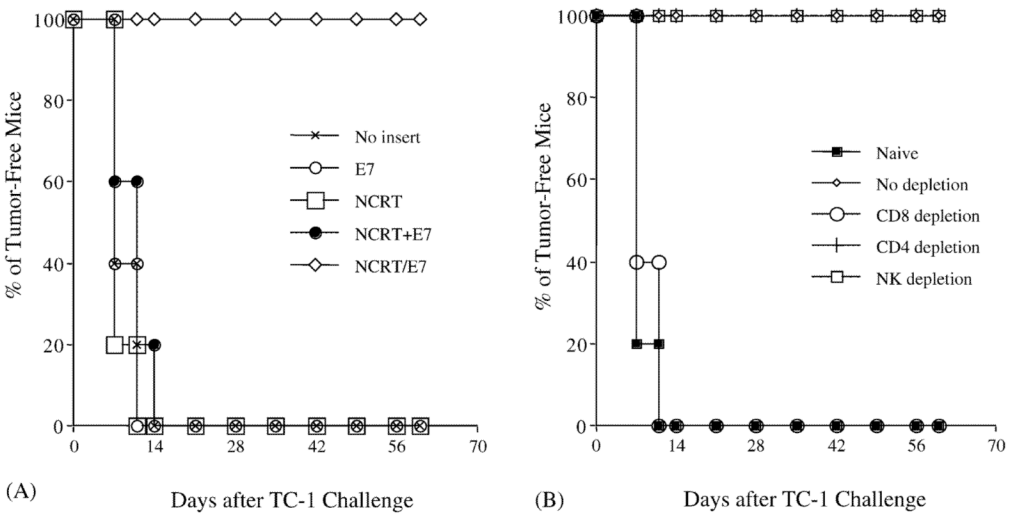

Fig. 7.

In vivo tumor protection experiments in mice vaccinated with various DNA vaccines and in vivo antibody depletion experiments in mice vaccinated with NCRT/E7. (A) Mice were immunized with various DNA vaccines and challenged as described in the Section 2 to assess the antitumor effect generated by each DNA vaccine. (B) An in vivo antibody depletion experiment was performed to determine the effect of lymphocyte subsets on the potency of the NCRT/E7 DNA vaccine. Mice were vaccinated, challenged with TC-1, and depleted of the relevant subset of lymphocytes as described in Section 2. Note that depletion of $CD8^+$ T cells, but not of $CD4^+$ T cells or NK cells, led to significant tumor growth in NCRT/E7 DNA-vaccinated mice. The data from the antibody depletion experiments shown here are from one representative experiment of two performed.